CHAPTER IV
RESULTS AND DISCUSSION

The nomenclatures of all catalysts shown below are employed in the following chapters.

TA-clay	=	Terephthalate-pillared hydrotalcite-type clay
V-clay	=	Decavanadate-pillared hydrotalcite-type clay
Mo-clay	=	Heptamolybdate-pillared hydrotalcite-type clay
Mo-V-clay	=	Heptamolybdate-decavanadate-pillared hydrotalcite-type clay
Ion	=	Fe loaded on clay by ion exchange method
Imp1	=	Fe loaded on dried clay by impregnation method
Imp2	=	Fe loaded on calcined clay by impregnation method

4.1 Catalyst Characterization

This section shows the results of the characterization of the prepared catalysts.

4.1.1 X-ray Diffraction

4.1.1.1 TA –clay based catalysts

Molecular form studies of terephthalate anion indicated that organic anions containing an aromatic ring would be adequately large to properly separate the brucite layers of hydrotalcite for polyoxometalates exchange (Drezdzon,1988). XRD patterns of TA-clay based catalysts are shown in Figure 4.1. The (001) plane peak of fresh and dried TA-clay occurs at the 2Θ angle of 6.16°, which has the d-spacing value of 14.33 Å. The d-spacing of the terephthalate anion-pillared hydrotalcites mentioned above agrees well with the d-spacing of 14.4 Å calculated by assuming the aromatic ring is perpendicular to the brucite layers. Moreover, in order to preserve its structure as clay layers, TA-clay cannot be calcined at the temperature of higher than 350 °C, indicating by the disappearance of all major peaks. Fe was further loaded on the TA-clay by two different methods: ion exchange and

impregnation. The XRD pattern of Fe-TA-clay Impl catalyst is different from those of Fe-TA-clay Imp2 catalyst. XRD patterns of Fe-TA-clay Impl catalyst show two peaks at the 2Θ angle of 14.34 and 23.13° while these two peaks disappear in case of Fe-TA-clay Imp2 catalyst. The XRD patterns of Fe-TA-clay based catalysts show no peak for iron oxide. Regardless of loading method, Fe-loaded catalysts were no longer conformed to clay layers.

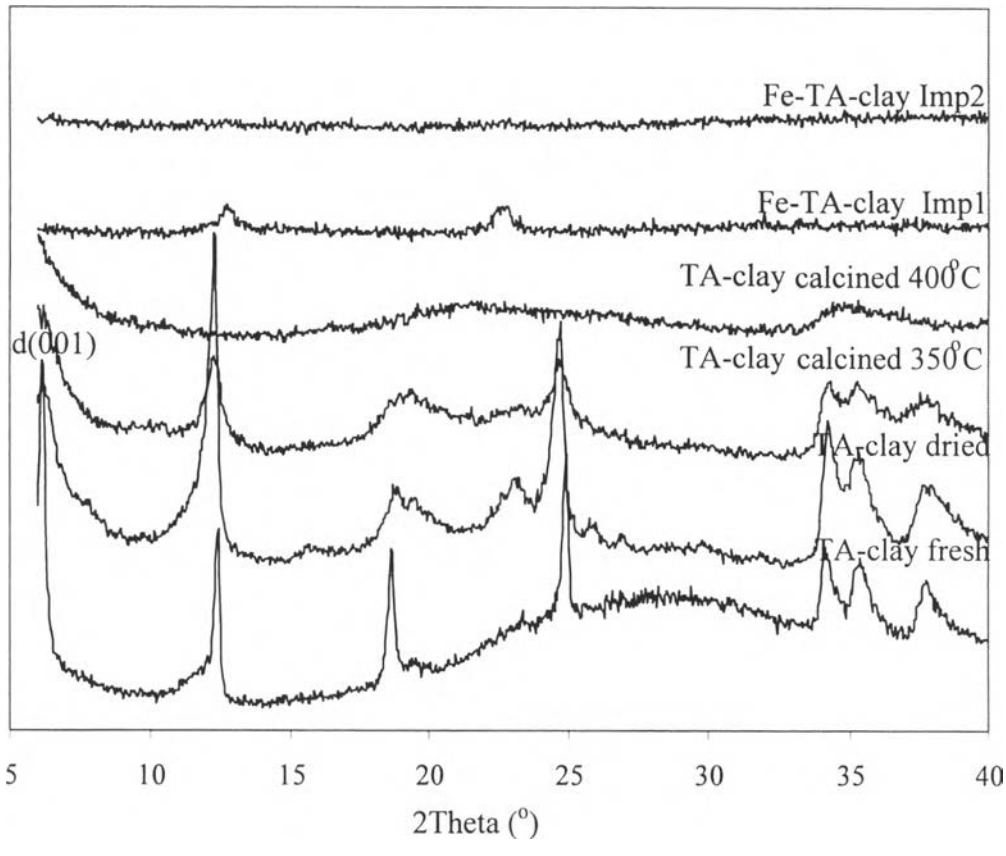

Figure 4.1 XRD patterns of terephthalate-pillared hydrotalcite-type clay.

4.1.1.2 V-clay based catalysts

Exchange of terephthalate-pillared hydrotalcite-typed clay with vanadate under mildly acidic conditions proceeded smoothly to yield decavanadate-pillared hydrotalcite-typed clay. Figure 4.2 shows XRD patterns of V-clay based catalyst. The (001) plane peak of dried V-clay appears at the 2Θ angle of 7.56°. The characteristic peak of (001) plane at the 2Θ angle of 6.16° is extreamly small. The d (001) is 11.68 Å. Furthermore, when V-clay layers was calcined at 350°C, the new two peaks appear at the 2Θ angle of 18.76° and 34.44° and its structure are collapsed at the calcination temperature of higher than 350°C. These two peaks represent aluminium oxide (Al_2O_3) and AlV_2O_4 when matched with JCPDF files. The d-spacing of decavanadate-pillared hydrotalcite (d = 11.9 Å) corresponds to a $V_{10}O_{28}^{6-}$ orientation in perpendicular to the brucite layers. Fe was loaded onto V-clay by two different methods: impregnation and ion exchange. The XRD patterns of Fe loaded catalysts of V-clay are different from unloaded V-clay catalysts. All major peaks indicating clay layer characteristics disappear. Again, Fe-loaded-V-clay catalysts were not anymore in form of clay layers.

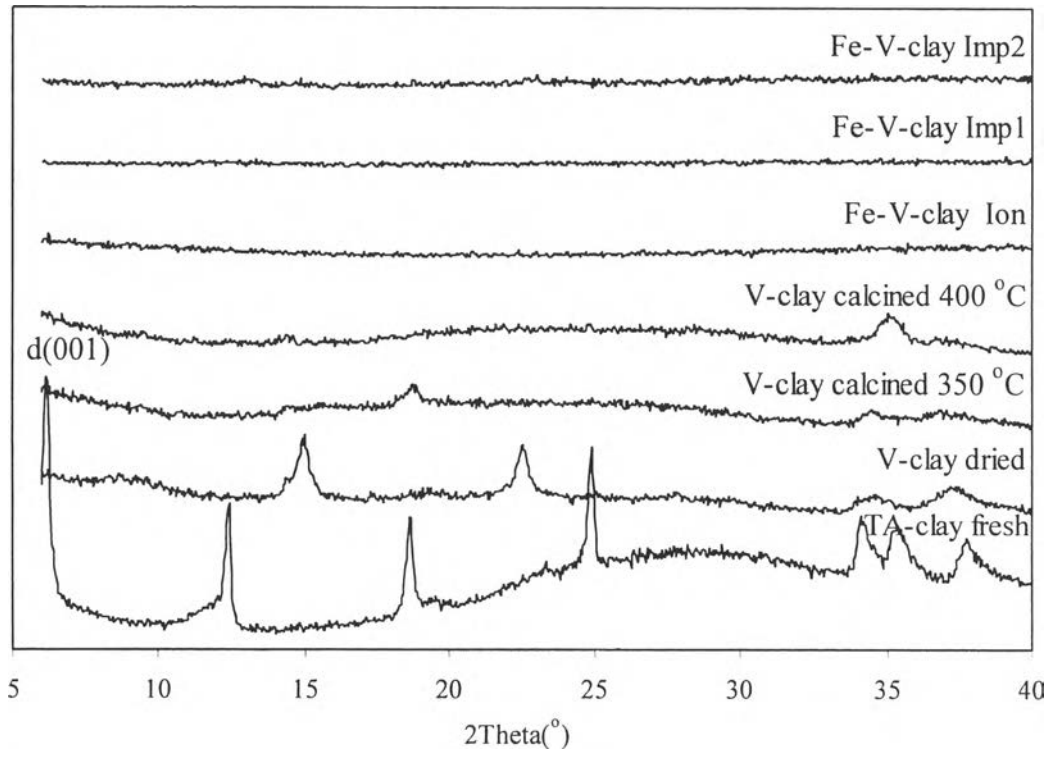

Figure 4.2 XRD patterns of decavanadate-pillared hydrotalcite-type clay.

4.1.1.3 Mo-clay based catalysts

Dried Mo-clay has the (001) plane peak at the 2Θ angle of 7.08° with the d-spacing value of 12.47 Å, and the main clay characteristic peak vaguely appears. After calcination at the temperature of higher than 350°C, this peak does not occur anymore, but there is a new peak at the 2Θ angle of 18.8° that represents $MgAl_3O_4$ and $Mg(OH)_2$ when matched with JCPDF files. The XRD patterns of Mo-clay clay based catalysts clearly indicate that the clay characteristic disappears as shown in Figure 4.3. XRD patterns of Fe-loaded Mo-clay catalysts roughly look alike, and indicate a highly amorphous form of the mixed oxide catalysts. However, no peak for iron oxide was observed from the XRD patterns of Fe-Mo-clay based catalysts.

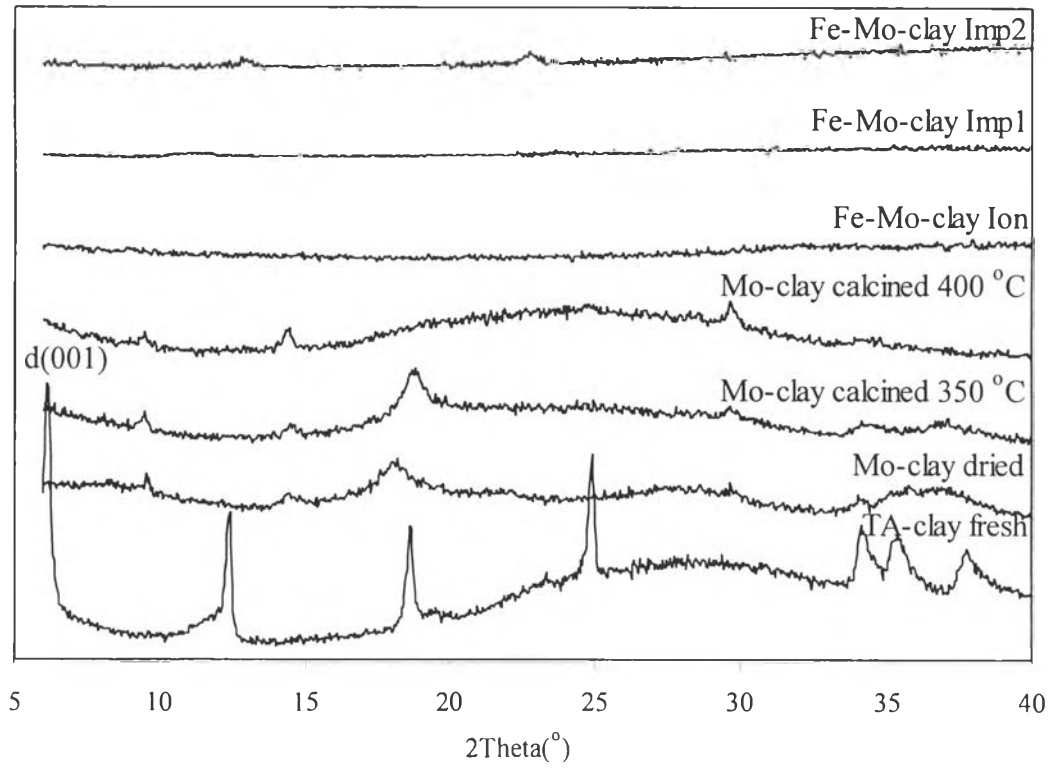

Figure 4.3 XRD patterns of heptamolybdate-pillared hydrotalcite-type clay.

4.1.1.4 Mo-V-clay based catalysts

Figure 4.4 illustrates the XRD patterns of Mo-V-clay based catalysts. The (001) plane peak of dried Mo-V-clay occurs at $2\Theta = 9.56^{o}$, which has the d-spacing value of 9.24 Å, but the clay characteristic peak does not appear. Futhermore, the (001) plane peak of V-clay and Mo-clay catalysts at the 2Θ angle of 7.56^{o} and 7.08^{o} with the d-spacing value of 11.68 Å and 12.47 Å, respectively also occur, but were not clearly observed. When Mo-V-clay was calcined at 350°C, the XRD patterns show the new peak at the 2Θ angle of 18.88^{o} which represents $MgAl_2O_4$ and AlV_2O_4 form JCPDF files. Because the d(001) peak for Mo-V-clay was changed to the 2Θ angle of 9.56^{o}, this observation means there was mixed oxide of polyoxometalates occurred. This results in the lower d-spacing (9.73 Å). The XRD patterns of Fe loaded Mo-V-clay cartalysts are different from those of Mo-V-clay clay based catalysts. Futhermore, there was still no peak for iron oxide. The reason why there was no peak of iron oxide in all catalysts because the Fe content is too small when compared to other components in any clay based catalysts.

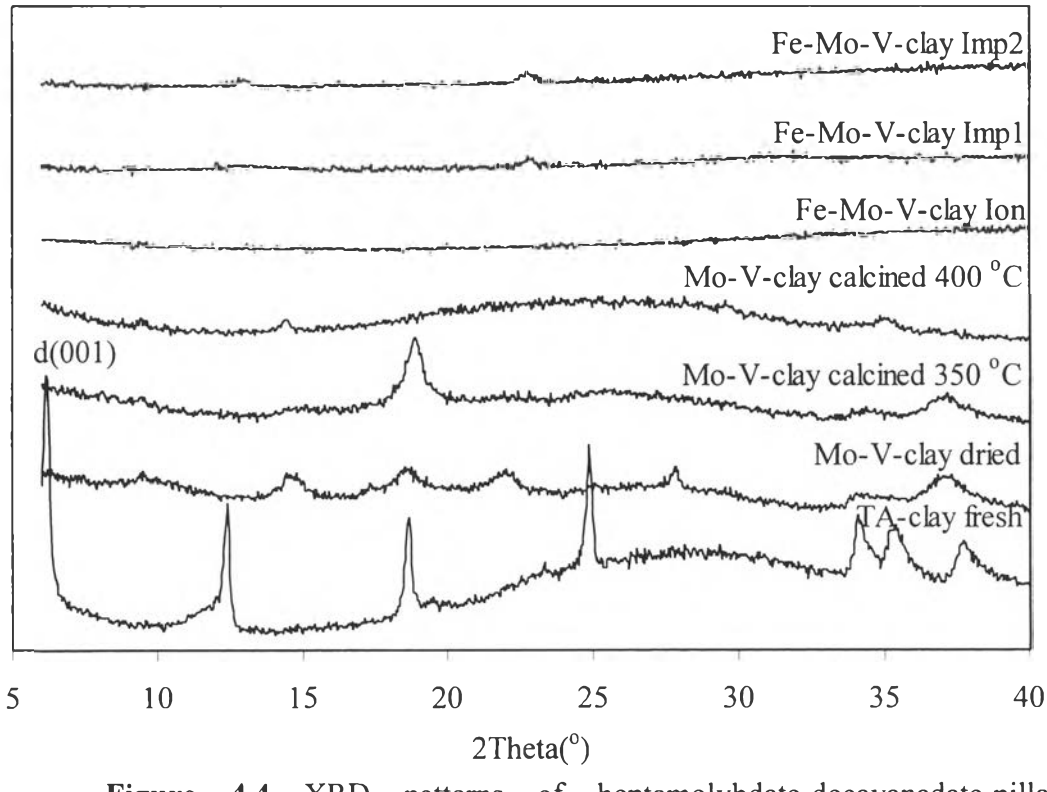

Figure 4.4 XRD patterns of heptamolybdate-decavanadate-pillared hydrotalcite-type clay.

4.1.2 BET Surface Area, Total Volume and Average Pore Diameter

BET surface areas, total pore volume, and average pore diameter of all studied catalysts are tabulated in Appendix A. The comparison of the surface area of all catalysts is shown in Figure 4.5.

Among unloaded catalysts, whose the surface area is between 39.45 and 68.51 m^2/g and the pore volume that is in range of 0.04 - 0.12 cc/g, the TA-clay catalyst shows the highest value of surface area. The average pore diameters of all Fe-unloaded catalysts are between 47 and 73 Å, and the TA-clay catalyst also has the largest pore.

The surface areas, pore volume, and average pore diameter of Fe^{3+} ion-exchanged catalysts are quite equal to those of the Fe-impregnated ones in both groups. Fe-Mo-clay catalyst shows the highest value for both surface area and pore volume in case Fe was loaded by ion exchange method. The values of surface area, pore volume and pore diameter of iron loaded catalysts by ion exchange method are between 73.3 – 110.6 m^2/g, 0.04 - 0.18 cc/g, and 63 - 70 Å, respectively. In case of impregnation method, Fe-loaded (on dried clay) catalysts have higher surface area than those loaded on calcined clay. Fe-V-clay catalyst shows the highest surface area of 116.1 m^2/g among all Fe-impregnation catalysts. Normally, surface area increases when a metal is doped on a catalyst. From the data, Fe^{3+} ion-exchanged Mo-clay catalyst has quite higher surface area than Mo-clay catalyst itself. However, this is still true for the case of Fe loading by impregnation method because its surface area is also not much higher when loaded with Fe. Iron may be mixed with molybdenum creating new phases possibly resulting in the small increase of surface area. Fe-loaded catalysts by impregnation have the values of pore volume in range of 0.06 – 0.13 cc/g and the average pore diameter between 40.9 and 57.1 Å.

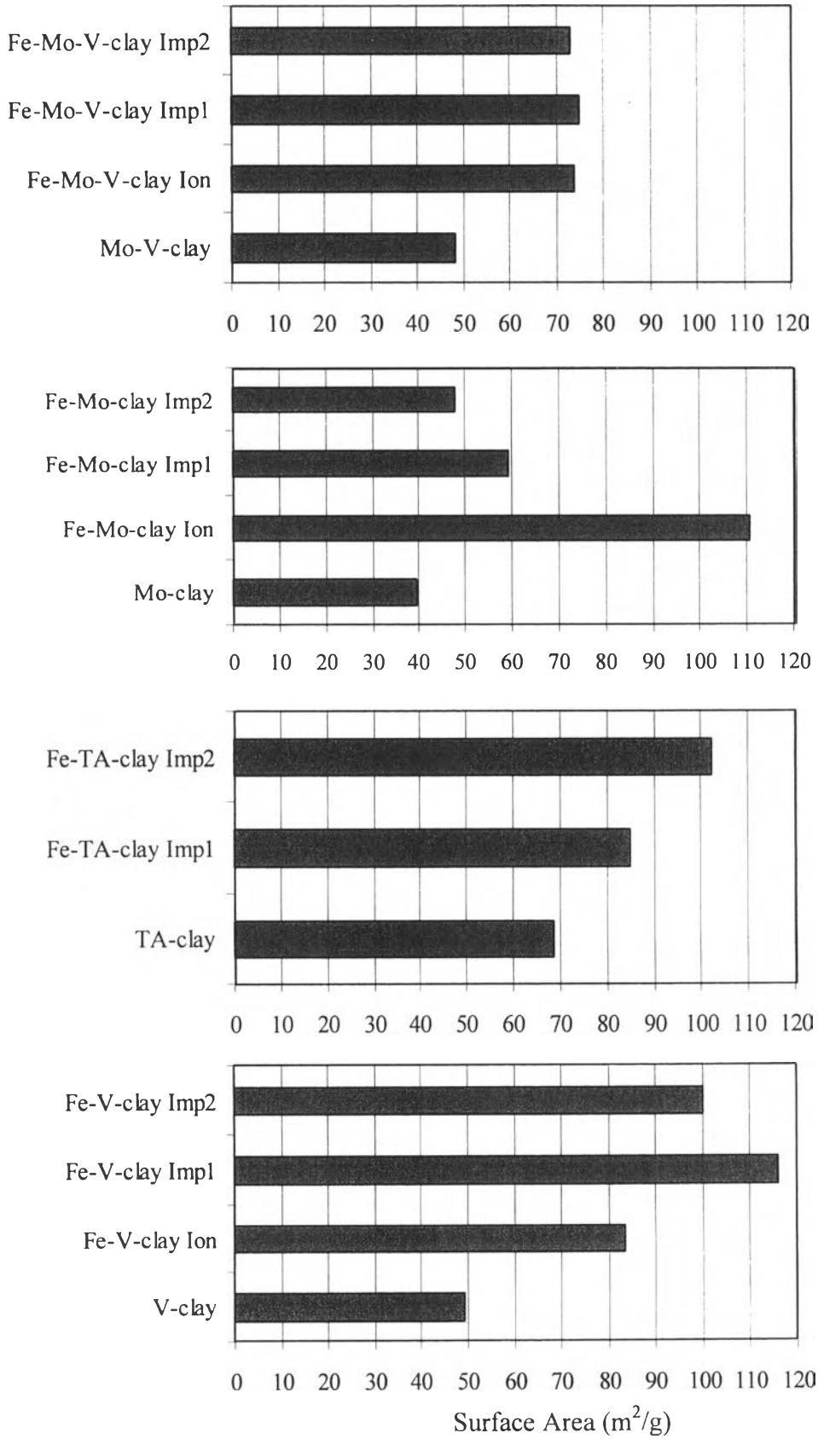

Figure 4.5 The surface area comparison of all catalysts.

4.1.3 Transmission Electron Microscopy

The clay layers of catalysts were visualized by using transmission electron microscope (TEM). The TEM images of these samples may not be clearly seen due to the limitation on specification of the machine, however, the layered structure could still be seen as depicted in Figure 4.6. The d-spacing of clay layers can be roughly measured. The d-spacing estimated from TEM micrographs approximately agree reasonably well with d-spacing determined by X-Ray diffraction.

Figure 4.6 Transmission electron micrographs of (a) TA-clay catalyst at 150,000X magnification, and (b) Mo-V-clay catalyst at 150,000X magnification.

4.1.4 Scanning Electron Microscopy

The surface morphology of the catalysts was studied by using SEM. The secondary electron images for both dried and calcined catalysts are shown in Figure 4.7. TA-clay catalyst was found to contain slightly flattened beadlike particle approximately 1000-2000 Å in diameter. The images of others catalysts illustrate the same surface morphology. After all catalysts were calcined, their surface appeared to be denser because water located between clay sheets was lost.

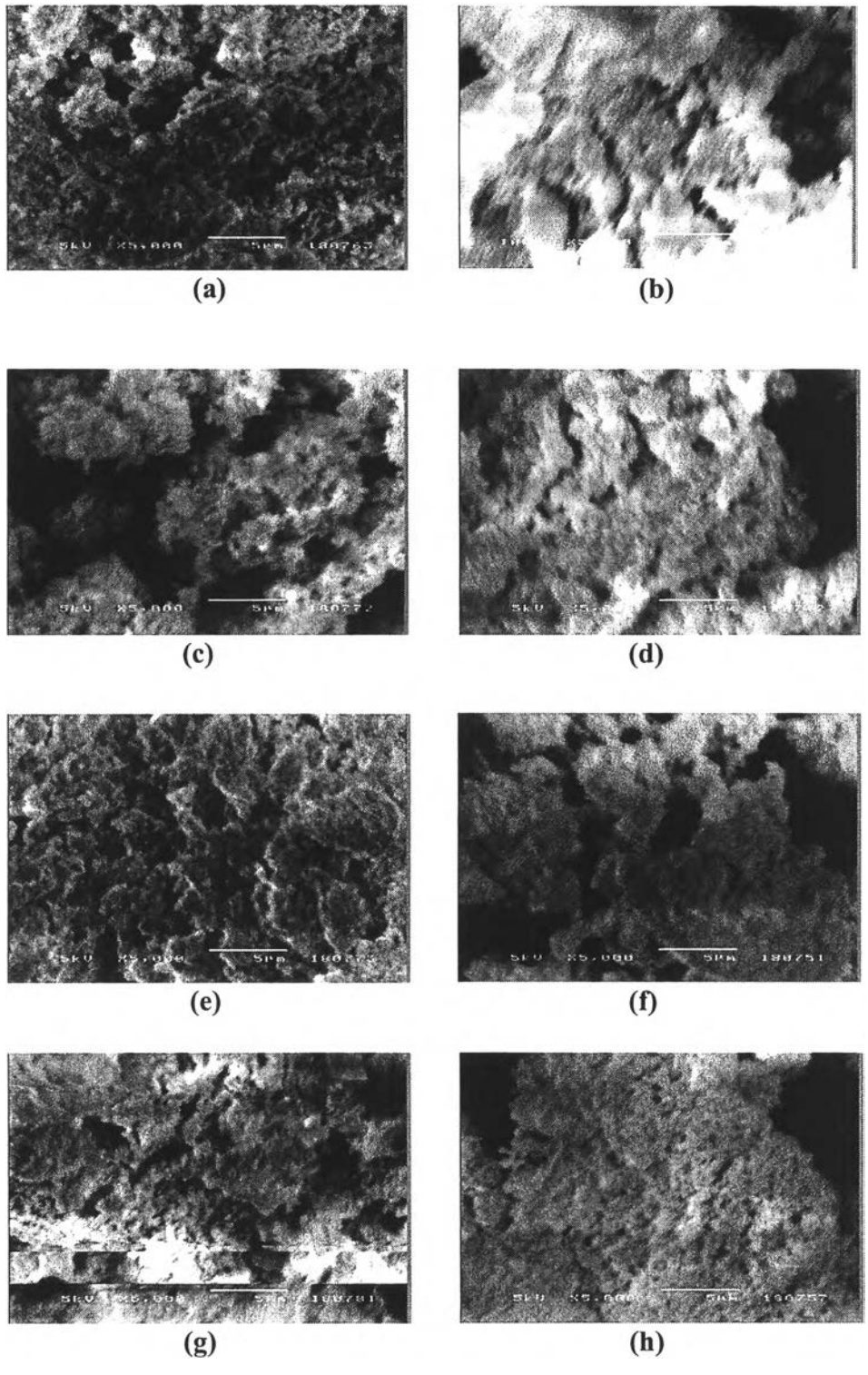

Figure 4.7 Scanning electron micrographs at 5000X magnification of (a) TA-clay dried, (b) TA-clay calcined at 350°C, (c) V-clay dried, (d) V-clay calcined at 350°C, (e) Mo-clay dried, (f) Mo-clay calcined at 350 °C, (g) Mo-V-clay dried, and (h) Mo-V-clay calcined at 350 °C.

4.1.5 Atomic Absorption Spectroscopy (AAS)

The amount of iron loaded on catalsyts was investigated and confirmed by using atomic absorption spectroscopy. In this study, all catalysts were loaded using $Fe(NO_3)_3.9H_2O$ solution to acheive 5 % weight of Fe. Fe^{3+} exchange capacity on all clay catalysts was also determined by AAS as shown in Figure B.1 in Appendix B. All polyoxoanion-pillared catlysts have the similar Fe^{3+} exchange capacity of around 8% Fe by weight. Therefore, the amount of 5 % Fe loaded on catalysts account for about 62.5% of full exchange capacity. It is noted in Figure B.1 that the exchange capacity graph of Mo-clay catalyst shows another plateau beyond the full exchange capacity, or at high concentration of iron (III) nitrate solutions. The rise of the graph would possibly result from precipitation of Fe on catalyst surface at high concentrated acidic solutions, or might have occurred from exprimental error.

4.1.6 Thermal Gravimetric Analysis

Phase change in catalysts upon changing temperature was investigated by thermogravimetry technique. The transition weight loss of the catalysts from TGA is shown in Figure 4.8. The weight loss appears in three zones: interlayer water loss, brucite layer deoxylation, and well maintained region. In the first zone, water located between interlayers of clay sheets was lost when the temperature was increased toward and beyond its boiling point. The first transition occurred around 350°C due to rearrangement of oxide surface on brucite layers in addition to loss of water, carbondioxide, and some organic compounds. In the second zone beyond the first transition, clays might have started to lose their layer structure until the second transition at 580°C where the clays might have completely lost the structure and become mixed oxides. This observation corresponds to the XRD patterns, showing no peaks of all clays when calcined at temperature higher than 350°C. When the temperature was higher than 580°C, the final structures were maintained. Catalyst weight was no longer changed in this region. By matching XRD patterns of both decavanadate clay and heptamolybdate clay with JCPDF files, the catalysts contained the combination of phases such as dominant α-$MgMoO_4$ and spinel phases, corresponding to those previously reported by Drezdzon (1988).

Figure 4.9 illustrates the weight loss patterns of Fe-loaded catalysts, which are similar to those unloaded ones. Fe^{3+} ion-exchanged catalysts lost their weight upon changing temperature more than those impregnated ones did. The weight loss patterns of Fe-impregnated catalysts are shown in Figure 4.10. Moreover, Fe-impregnated (on dried clay) catalyst lost their weight higher than Fe-impregnated (on calcined clay) catalyst, because they were calcined once. TA-clay based catalysts tend to have high weight loss because they carry large amounts of water between clay layers.

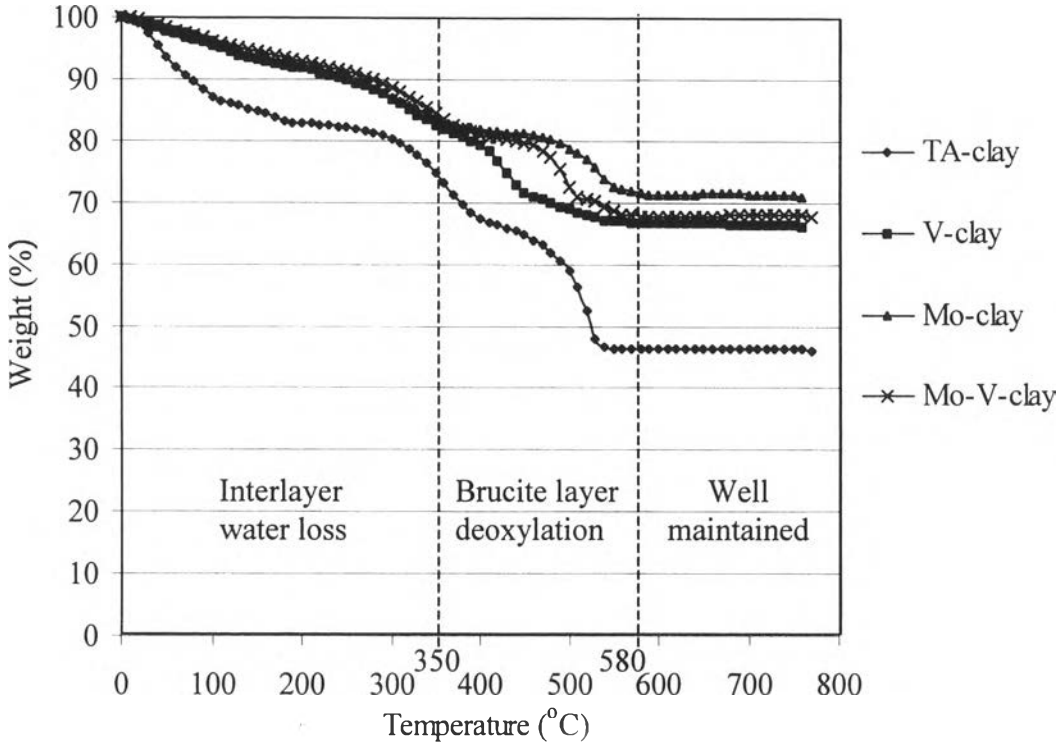

Figure 4.8 The transition weight loss of Fe-unloaded catalysts from thermalgravimetric analysis.

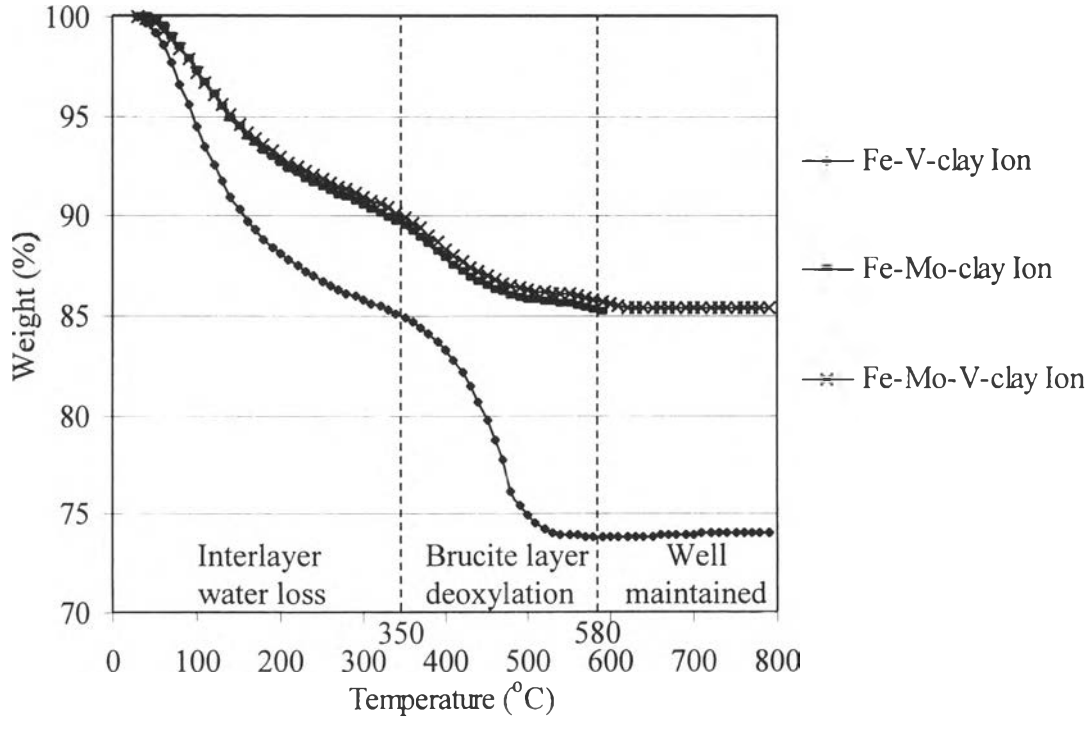

Figure 4.9 The transition weight loss of Fe^{3+} ion-exchanged catalysts.

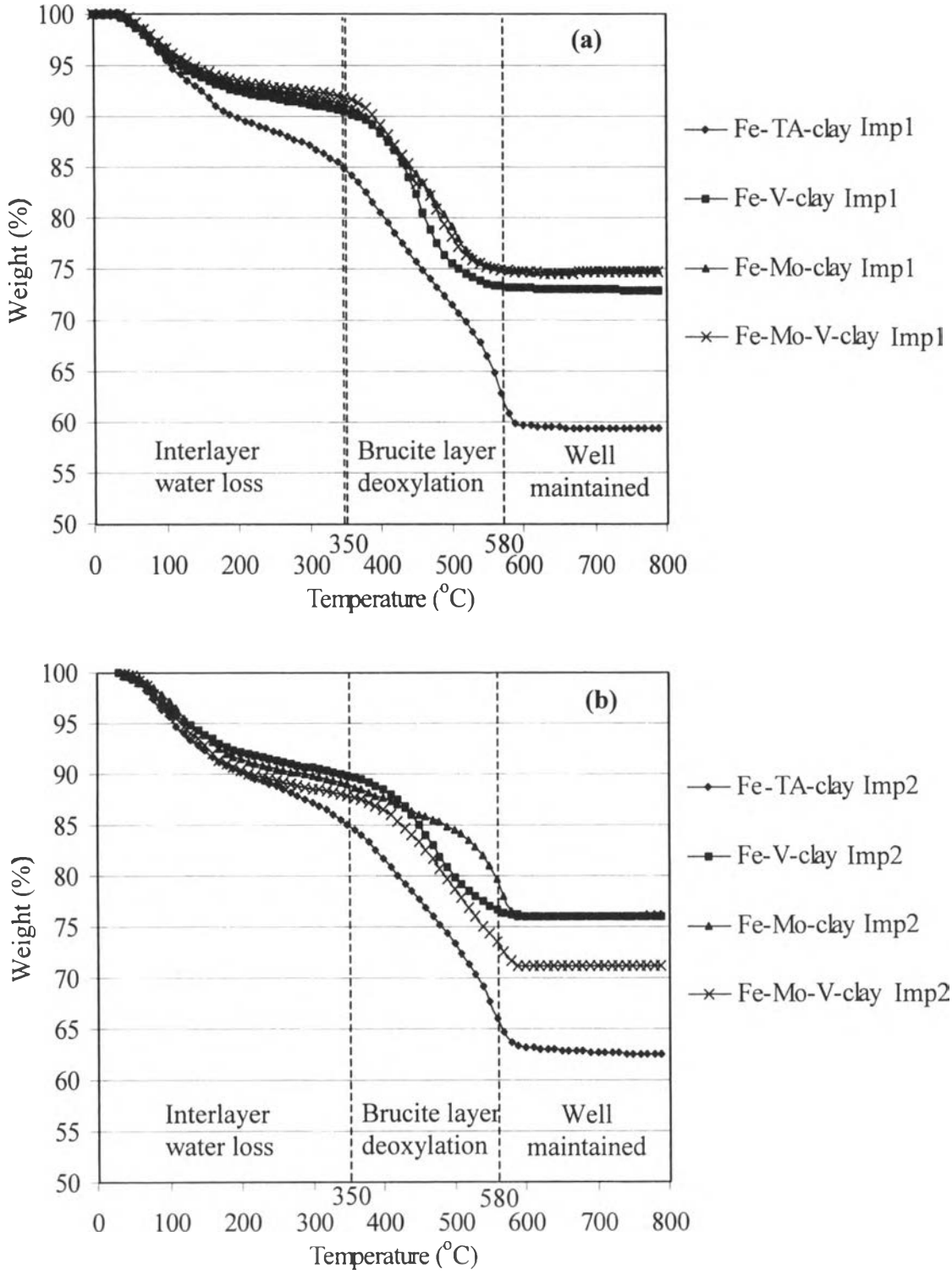

Figure 4.10 The transition weight of Fe-impregnated catalysts by:
(a) on dried clay, and (b) on calcine clay.

4.1.7 Temperature Program Desorption

NO adsorption and/or desorption was carried out by temperature program desorption to study the NO adsorption capacity of catalysts for both unloaded and Fe-loaded ones. NO desorption signal was detected by mass spectroscopy with the m/z of 28. Normally, in TPD experiments, when a probe molecule adsorbs on a surface, it will desorb with the same amount, and area under TPD curve corresponds to the amount of adsorbed component. However, in the case, NO as a probe could react with oxygen on the oxide surface, producing other molecules from oxidation products during the TPD experiments as detected by Mass Spectrometer. Therefore, area under TPD curve, for this case, actually corresponds to the amount of desorbed NO, not exactly the amount of NO adsorbed on the surface at the beginning, because NO has been partially dissociated. A large area under curve would mean (1) a large amount of NO desorbed, reflecting a large adsorbed amount as well, or (2) possibly, a little amount of NO dissociated. On the other hand, a small area under curve would reflect (1) a small amount of NO adsorbed, or (2) possibly, a large number of NO dissociated.

From the TPD results of unloaded catalysts shown in Figure 4.11, TA-clay shows the largest amount of NO desorbed due to the highest d-spacing between clay layers. While V-clay, Mo-clay and Mo-V-clay catalysts have NO desorbed in comparable amounts, but much smaller than those of TA-clay one. The TA-clay catalyst can adsorb a large amount of NO, leading to a high chance to be a good NO adsorbent. NO desorbed from V-clay and Mo-V-clay catalysts at lower temperatures than TA-clay catalyst. This observation means that NO adsorption on V-clay and Mo-V-clay catalysts was not as strong as on TA-clay catalyst. In contrast, Mo-clay had NO desorbed at the highest temperature. This result refers that NO was more strongly adsorbed on Mo-clay catalyst than on the others. The observations indicate that NO could be dissociated easily according to the following order: V-clay > Mo-V-clay > TA-clay > Mo-clay.

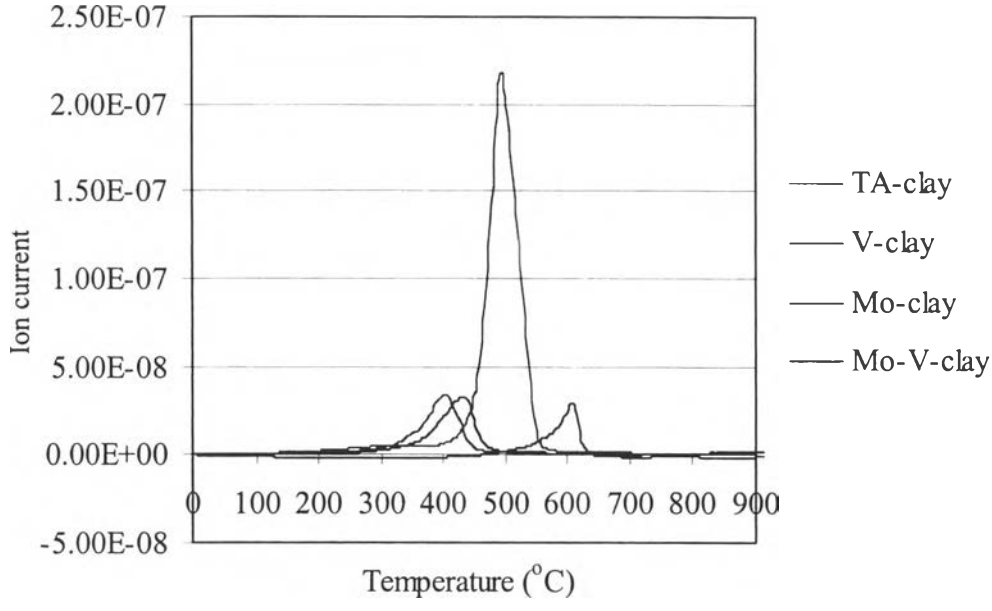

Figure 4.11 TPD results of NO desorption of all unloaded catalysts.

Figure 4.12 shows TPD results of NO desorption from Fe^{3+} ion-exchange catalysts. The amounts of NO desorbed from Fe^{3+} ion-exchanged catalysts were clearly much smaller than those from the unloaded catalysts, also indicating a small amount of NO adsorbed. However, NO desorption from Fe^{3+} ion-exchanged catalysts occurred at slightly lower temperatures than that from the unloaded catalysts.

NO desorbed from Fe-V-clay catalyst at the lowest temperature, among other from Fe^{3+} ion-exchanged catalysts. Fe-Mo-clay and Fe-Mo-V-clay catalysts show NO desorbed at higher temperature than Fe-V-clay catalyst, indicating that NO would rather adsorb on these two clay catalysts stronger than Fe-V-clay catalyst. Therefore, NO dissociation would occur most easily on Fe-V-clay catalyst.

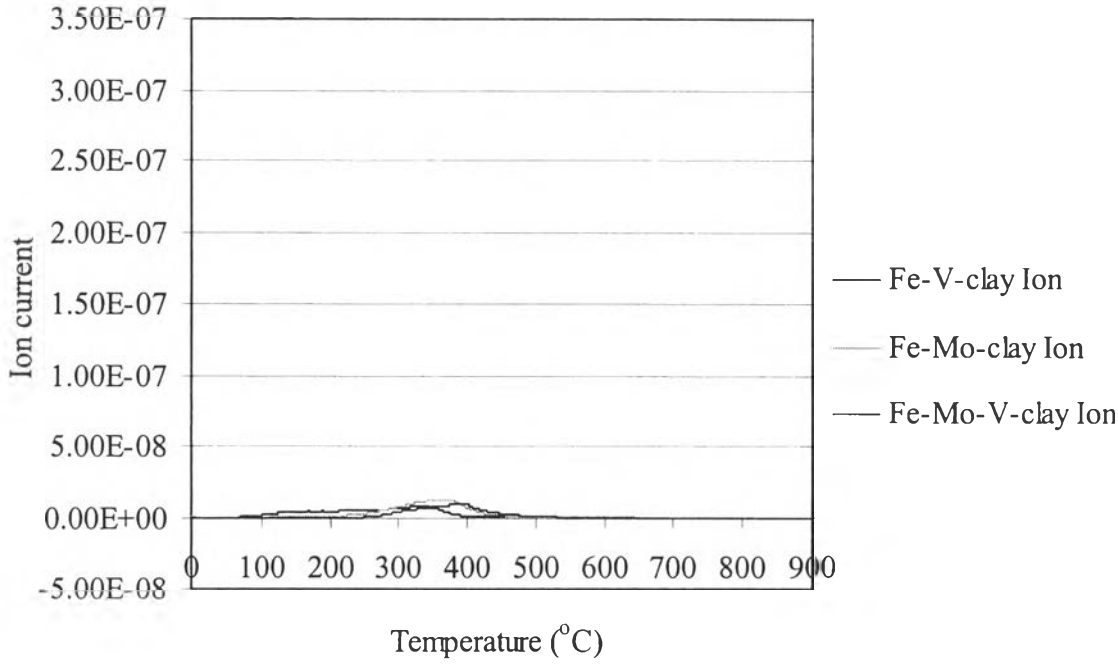

Figure 4.12 TPD results of NO desorption on Fe^{3+} ion-exchanged catalysts.

In case of Fe-impregnated catalysts, the catalysts with both Fe loaded on dried clay and Fe loaded on calcined clay gave almost the same TPD patterns as shown in Figure 4.13. Fe-TA-clay catalyst showed the highest amount of NO desorbed at the temperature of around 450°C. NO desorbed in the smallest amount from Fe-V-clay catalyst at lower temperature. Fe-Mo-clay and Fe-Mo-V-clay catalysts have significant higher amount of NO desorbed than Fe-V-clay catalyst, but the adsorption occurs at high temperature. Therefore, Fe-TA-clay catalyst should have a better chance to have NO conversion than others due to the large amounts of NO adsorbed. NO would be dissociated on Fe-V-clay catalyst.

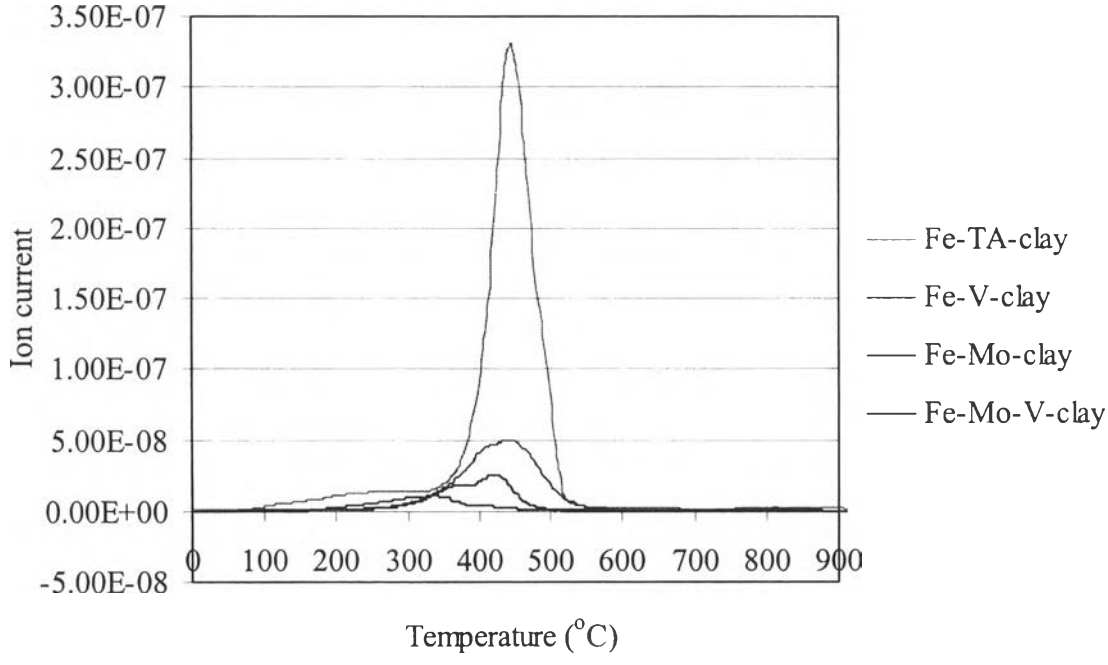

Figure 4.13 TPD results of NO desorption of Fe-impregnated catalysts.

In the TPD experiments, only NO employed as a probing molecule was adsorbed on the surface without co-adsorption of NH_3 and O_2 used as co-reactants in the activity testing. However, in this work, TPD of NO could only indicate how much NO is adsorbed and how easily NO is dissociated. Therefore, the product selectivity could not be compared with that from the activity testing.

4.2 Catalytic Activity Testing

The reactant mixture containing 1000 ppm NO, 1000 ppm NH_3, 2% O_2 balanced with helium was fed to the reactor with the GHSV of 226,000 l/h at 350 °C. The conversion was determined when NO concentration in the feed was constant.

4.2.1 Unloaded Catalysts

Mo-V-clay catalyst showed the highest activity at 75.5% NO conversion under the above conditions. TA-clay itself used as the support of all catalysts gave the high NO conversion of around 65 %. Moreover, V-clay and Mo-clay catalysts also showed relatively the same NO conversion as TA-clay did. Therefore, intercalation of individual polyoxomolybdate and polyoxovanadate anions did not improve the activity. However, if two types of polyoxoanions were co-intercalated in the clay layers, the conversion of NO was improved about 15%. The increase in conversion would indicate the synergistic effect between Mo and V. NO conversion of all unloaded catalysts is shown in Figure 4.14 and listed in Table B.18 in Appendix B.

N_2 selectivity of all unloaded catalysts is shown in Figure 4.15 and listed in Table B.18 in Appendix B. Although Mo-V-clay catalyst was the highest activity catalysts, it is the least selective and as selective as Mo-clay catalyst. The N_2 selectivity was about 30%. Polyoxomolybdate anions intercalated into the clay layer seemed to reduce N_2 selectivity. The V-clay catalyst also showed 61.6% of N_2 selectivity, which was the highest N_2 selectivity among three unloaded catalysts. TA-clay had only moderate N_2 seletivity which was about 30%.

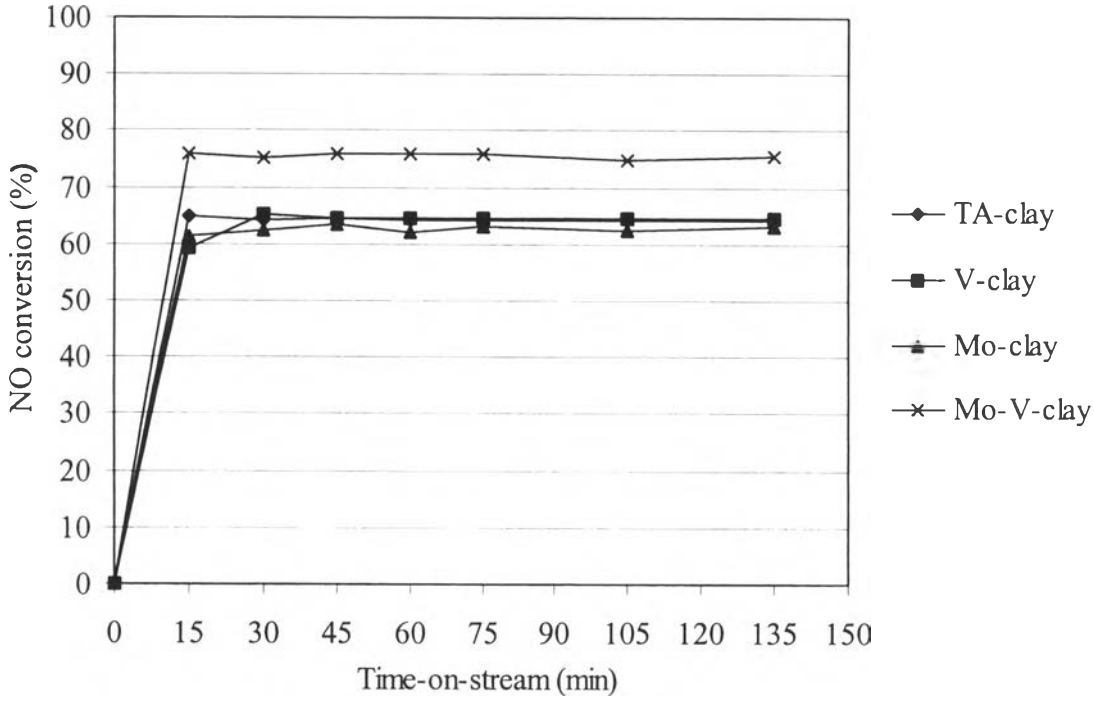

Figure 4.14 NO conversion of unloaded catalysts.

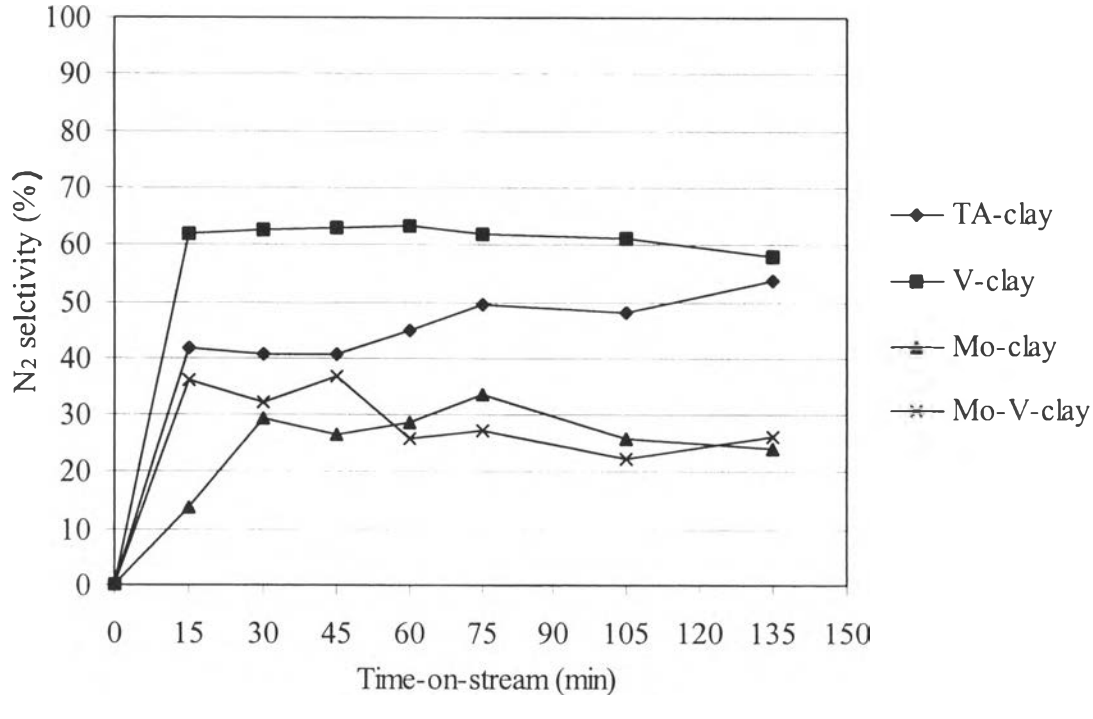

Figure 4.15 N_2 selectivity of unloaded catalysts.

4.2.2 Fe-loaded Catalysts

All Fe loaded catalysts were tested under the same conditions as used in the previous section. In all cases, 100% N_2 selectivity was achieved which obviously resulted from Fe-loading, regardless of the loading method. However, NO conversion was generally lower than those of unloaded catalyst.

4.2.2.1 *Fe^{3+} ion-exchanged catalysts*

Fe^{3+} ion-exchanged V-clay catalyst gave the highest NO conversion of about 28%, while Fe^{3+} ion-exchanged Mo-clay and Fe^{3+} ion-exchanged Mo-V-clay catalysts had two times lower conversion. Synergy between Mo and V in these cases was not observed. Figure 4.16 illustrates NO conversion of Fe-loaded catalysts by ion exchange method.

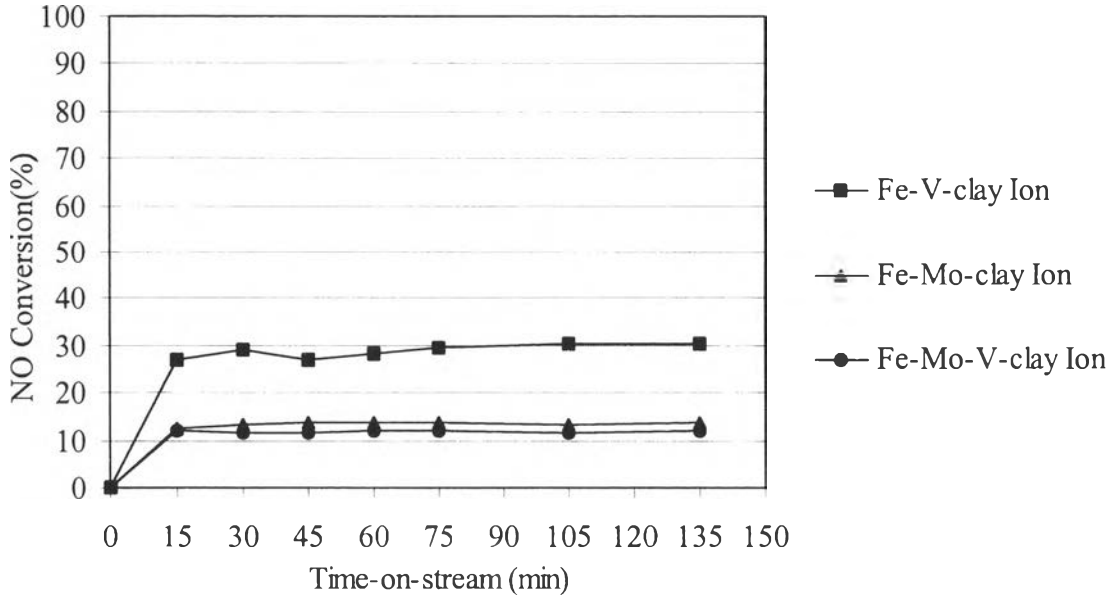

Figure 4.16 NO conversion of Fe^{3+} loaded catalysts prepared by ion exchange method.

4.2.2.2 *Fe-impregnated catalysts*

Figure 4.17a and b illustrate NO conversion of Fe-impregnated catalysts with Fe loaded on dried clay and on calcined clay, respectively. All Fe-impregnated catalysts gave extremely low conversion of about 10% or less, except the case when Fe was impregnated on calcined TA-clay catalyst whose NO conversion was about 28%. Regardless of the loading sequences, impregnation method seemed not to be the appropriate method of Fe loading in these cases.

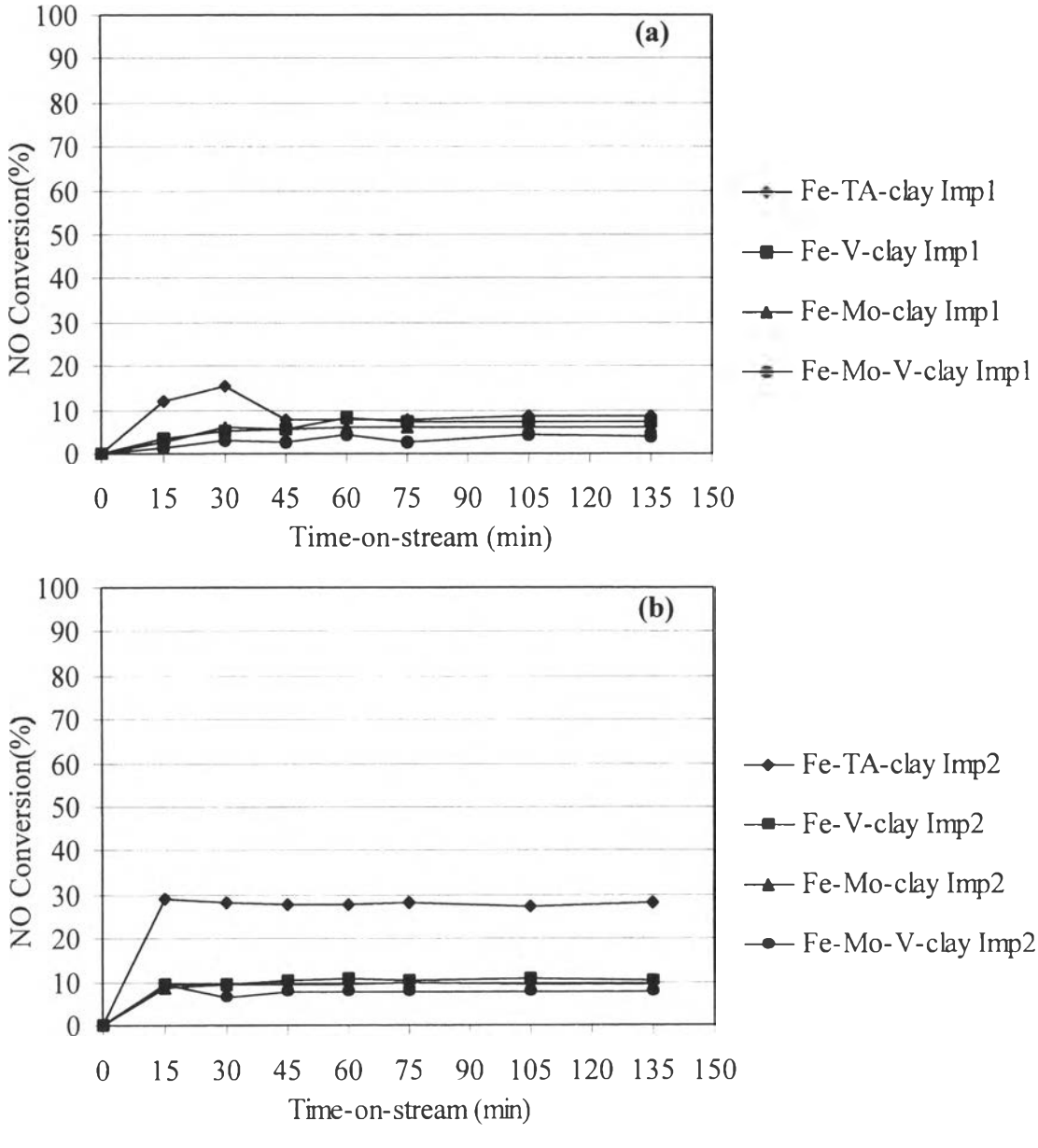

Figure 4.17 NO conversion of Fe-loaded catalysts prepared by imprenation (a) on dried clay, and (b) on calcined clay.

The reaction results showed that Fe-loaded catalysts by ion exchange method had higher yield than the catalyst prepared by impregnation method. Therefore, ion exchange seems to be a good method for loading metals potentially selective to N_2 production. Raw data of catalytic activity testing were attached in Appendix B.

Possibly, loading metals on catalyst could result in higher selectivity, but it does not always increase catalytic activity, therefore, consideration of which procedure and how to load metal is important. The method of metal loading can affect the catalytic activity, because it relates to their physicochemical properties of catalysts such as, surface area and adsorption-desorption. Fe-loaded catalysts by ion exchange method, exhibited high surface area due to Fe^{3+} replacement with some protons on clay structure. Additionally, NO also desorbed in large amount at low temperature. These characteristics lead them to have high NO conversion. On the other hand, Fe impregnated on catalysts might have plugged the pores, thus lowering the surface area, and then decreasing activity of the catalyst although it might be selective to N_2.

4.2.3 Comparison among All Catalysts

NO conversion, N_2 selectivity, and N_2 yield of all pillared hydrotalcite-type clay catalysts are compared in Figures 4.18, 4.19, and 4.20, respectively. The unloaded catalysts gave significantly higher NO conversion, but lower N_2 selectivity than Fe-loaded ones. Consequently, the catalysts can be classified into two groups: one with high conversion and another with high selectivity. In order to correctly compare among catalysts, yield of N_2 must be employed as criterion. As shown in Figure 4.20, the V-clay catalyst gave the highest yield. Mo intercalated in the layers of TA-clay did not improve the yield. The synergistic effect between Mo and V was insignificant because the addition of Mo and V did not improve the yield. Fe^{3+} ion-exchanged V-clay catalyst can potentially be further improved since it gave quite high yield.

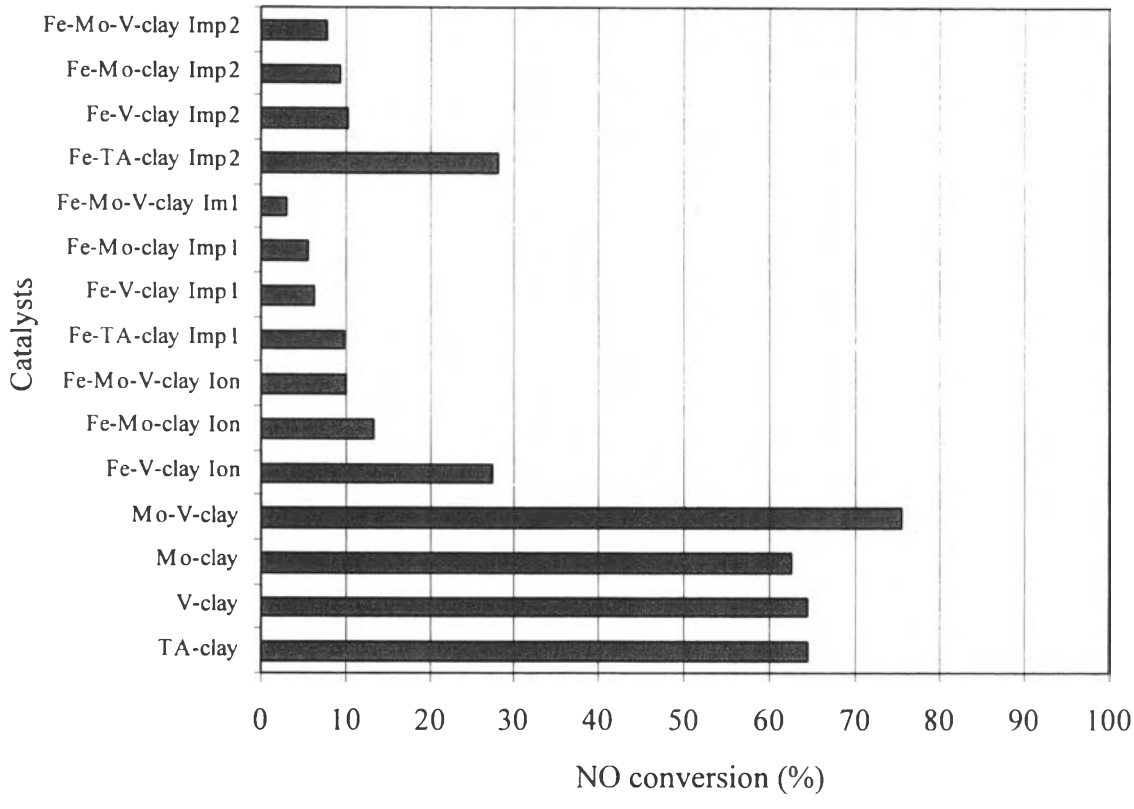

Figure 4.18 NO conversion of all pillared hydrotalcite-type clay catalysts.

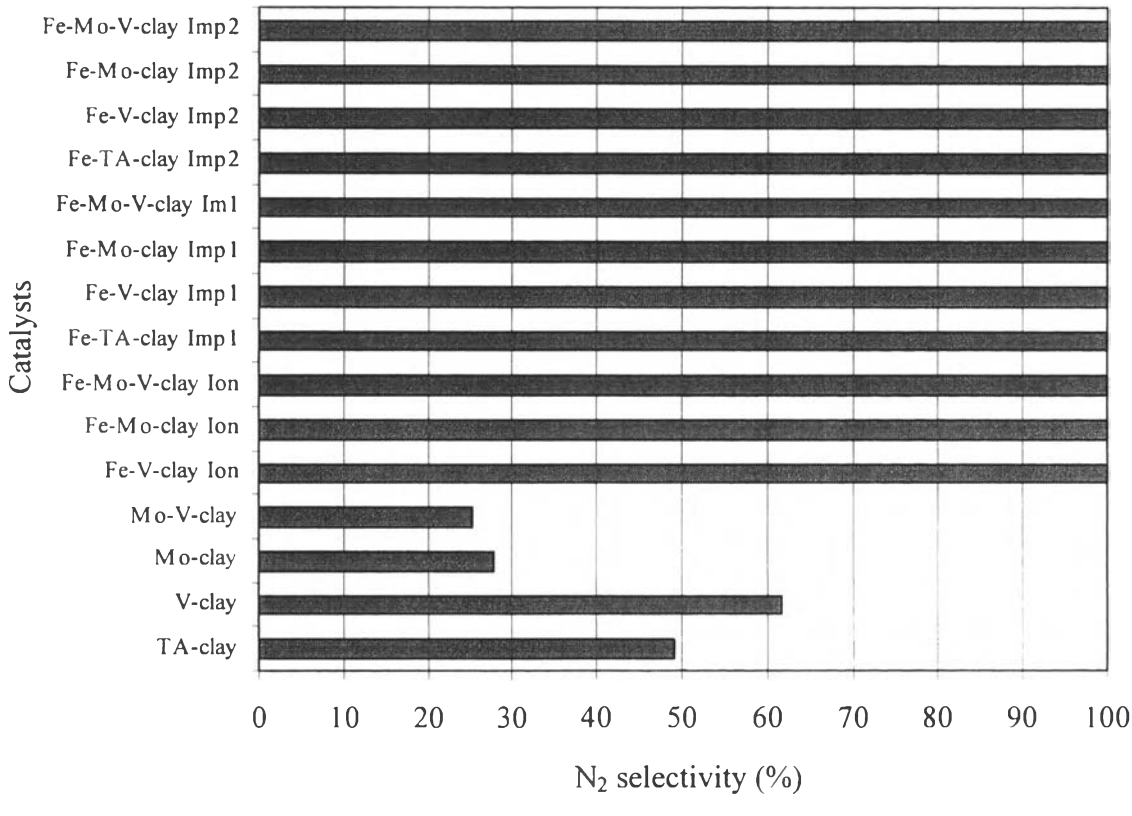

Figure 4.19 N_2 selectivity of all pillared hydrotalcite-type clay catalysts.

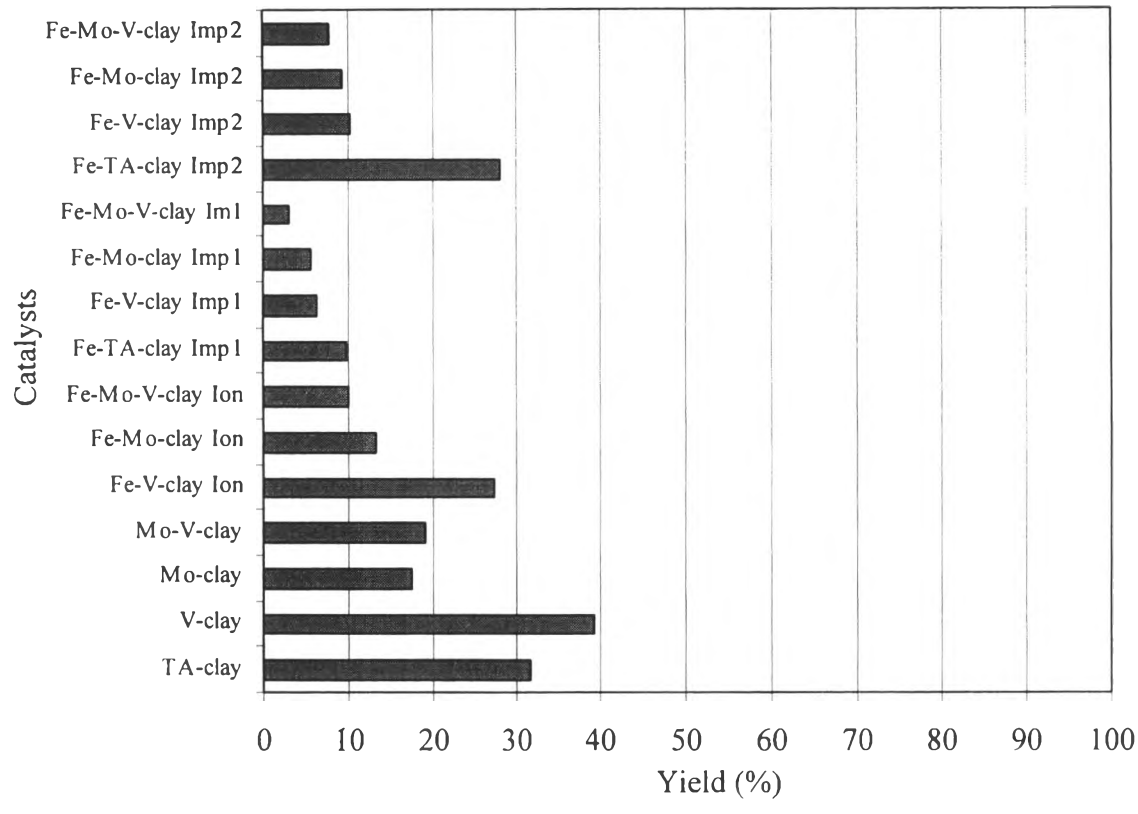

Figure 4.20 Yield of all pillared hydrotalcite-type clay catalysts.